IOP Publishing Physica Scripta
Phys. Scr. 95 (2020) 035404 (14pp) https://doi.org/10.1088/1402-4896/ab520b

Particle confined in modified ring-shaped potential

Shalini Lumb Talwar[1], Sonia Lumb[2], K D Sen[3] and Vinod Prasad[4,5]

[1] Department of Physics, Maitreyi College, University of Delhi, New Delhi-110021, India
[2] Department of Physics and Electronics, Rajdhani College, University of Delhi, New Delhi-110015, India
[3] School of Chemistry, University of Hyderabad, Hyderabad-500046, India
[4] Departamento de Quimica, Universidad Autónoma Metropolitana, San Rafael Atlixco No. 186 Iztapalapa, 09340, Ciudad de Mexico, Mexico

E-mail: vprasad@ss.du.ac.in

Received 29 July 2019, revised 17 October 2019
Accepted for publication 28 October 2019
Published 6 February 2020

Abstract

The spectrum of a particle confined in Hulthén plus ring-shaped potential is obtained by solving the time-independent Schrödinger equation numerically. The effect of potential parameters on various properties of the particle have been investigated in detail. The energy levels, radial matrix elements, oscillator strengths and polarizabilities of the particle have been found to show strong dependence on the confining potential parameters. The presence of the ring potential is found to appreciably alter the angular part of dipole matrix elements. Also, it is shown that the comparison theorem of Quantum Mechanics for energy eigenvalues for four different potentials, viz., Coulomb, Hulthén, Yukawa and Hulthén2 is independent of the presence of ring potential.

Keywords: Hulthén potential, ring-shaped potential, comparison theorem, oscillator strength, polarizability

(Some figures may appear in colour only in the online journal)

1. Introduction

The Hulthén potential [1, 2] is one of the most important short-range potentials in physics and is extensively used to describe the bound and continuum states of the atomic interaction systems. It belongs to the class of screened Coulomb potentials [3–6] and has applications in a number of branches of Physics such as nuclear and particle physics, atomic physics, condensed matter physics, chemical physics and high energy physics ([7, 8] and references therein). This potential is very similar to Yukawa potential [9] as it assumes the form of Coulomb potential for small r and decays exponentially to zero for large r. The quantum mechanical equations with the Hulthén potential have been dealt with by a number of authors either analytically or numerically [7, 10–16].

The representative potentials for realistic physical systems may often deviate from the conventional spherical models like Coulomb, Yukava or Hulthén potentials [17–21]. Thus, angle-dependent potentials which refine such potentials serve as a new class of potentials. Such potentials are employed in the study of non-spherically symmetric problems that often occur in chemistry. A number of articles have been devoted to the study of non-central potentials [22–37].

Chen and Dong [31] introduced a new ring-shaped potential and solved the Schrödinger equation for the Coulomb plus the new ring-shaped potential analytically. This potential was further combined with Kratzer potential by Cheng and Dai [38] to propose a new potential. Also, approximate bound-state solutions with Hulthén plus ring potential for non-zero orbital angular momentum have been obtained by the conventional Nikiforov-Uvarov method [39]. The energy eigenvalues and the corresponding wave functions have been obtained by solving non-relativistic Schrödinger equation for Hulthén–Yukawa plus angle dependent potential using the generalized parametric form of Nikiforov-Uvarov method [32]. Analytical solutions of Schrödinger equation with the generalized Hulthén potential plus a new ring shaped potential have been obtained by Ikot *et al* [40].

[5] On leave from Department of Physics, Swami Shraddhanand College, University of Delhi, Delhi-110036, India.

The study of such non-central potentials has gained significance due to their wide range of applications in various fields like nuclear physics and quantum chemistry as they could be used to discuss the interactions between pair of nuclei and ring-shaped organic molecules such as cyclic polyenes and benzene [32]. The harmonic oscillator potential plus a novel angle-dependent potential has been employed to study the problem of the relativistic motion of a $1/2$-spin particle [34]. This potential suggested for the first time by Berkdemir [35] in the Schrödinger picture might be useful in studying the relativistic energy spectra and wave functions of ring-shaped molecules.

The various ring-shaped potentials have recently been used and explored in different contexts. For example, Amirfakhrian and Hamzavi [41] have studied solutions of Schrödinger equation with the Morse plus ring-shaped potential. They have detailed bound state energies of many diatomic molecules. Chen *et al* [42] have reported spin–orbit splitting of single and double ring-shaped potentials along with harmonic oscillator potential. They have reported accidental degeneracy in some special cases. The angle-dependent ring-shaped potential along with many radial coordinate dependent potentials have found new attraction in low-dimensional semiconductor systems [43–46]. A solution of the radial and angular parts of the Klein–Gordon equation for Pöschl–Teller double-ring-shaped Coulomb potential has been found by Hassanabadi *et al* [47]. Liu *et al* [48] have studied optical properties of 3D ring-shaped pseudoharmonic potential. They have solved the equation of motion of the system with separation of variables method. Khordad [49] has recently reported the analytical results to show the effects of spin–orbit and magnetic field on the energy levels of quantum dots [50] confined in ring-shaped potential. Chabab *et al* [51] have used this type of potential to study the spectra of triaxial nuclei. This type of ring-shaped potential has been further used along with other radial potentials to explore many physical aspects of confined quantum systems. Pure (unscreened) ring-shaped potentials have applications in many organic molecules. In molecular physics, this potential has attracted a lot of theoretical investigations. For example, the study of molecular diamagnetic susceptibility and other properties have been investigated [52].

The aim of the present work is to numerically solve the Schrödinger equation, equation (6), for a screened Coulomb Hulthén plus ring-shaped potential. It may be mentioned that the Schrödinger equation has been solved analytically for such potentials [32, 39, 40] but these solutions are worked out within the framework of approximation schemes to deal with the centrifugal term. In the present work a particle confined in Hulthén plus ring-shaped potential is considered and the corresponding Schrödinger equation has been directly solved with no approximation to the centrifugal term to obtain the energy eigenvalues and wavefunctions with a focus on studying its oscillator strengths and static polarizabilities. To the best of our knowledge, the present study has not been reported earlier in the literature. In this respect, this work presents novel results and complements the earlier interesting studies involving the useful model potentials [32, 39–41]. The presentation of our work is organized as follows. The related theoretical details are described in section 2 The results are discussed in section 3 This is followed by conclusions in section 4.

2. Theory

The Schrödinger equation for a particle confined in Hulthén plus ring-shaped potential in spherical polar coordinates is written as

$$\left(\frac{-\nabla^2}{2} + V(r,\theta)\right)\Psi_{nl'm}(r,\theta,\phi) = E\Psi_{nl'm}(r,\theta,\phi). \quad (1)$$

Atomic units are used throughout this paper, i.e. $\hbar = m_e = e = 1$. The potential $V(r, \theta)$ is given by

$$V(r,\theta) = -Z\alpha\frac{e^{-\alpha r}}{1-e^{-\alpha r}} + \beta\frac{\cos^2\theta}{r^2\sin^2\theta}, \quad (2)$$

where α is the screening parameter, β is a real constant and Z is the atomic number [39]. The second term in equation (2) is the ring shaped potential introduced by Chen and Dong [31]. Since this is the case of a non-spherically symmetric potential, subscript l' has been used for the wavefunction in equation (1) instead of l which is the usual angular momentum quantum number.

The usual separation of variables technique is applied for radial and angular parts by taking

$$\Psi_{nl'm}(r,\theta,\phi) = R_{nl'}(r)\gamma_{l'm}(\theta,\phi), \quad (3)$$

where

$$R_{nl'}(r) = U_{nl'}(r)/r \quad (4)$$

and

$$\gamma_{l'm}(\theta,\phi) = \Theta_{l'm}(\theta)\Phi_m(\phi). \quad (5)$$

Since this is the case of non-spherically symmetric potential, the usual notation for the spherical harmonics $Y(\theta, \phi)$ has been avoided. The Schrödinger equation reduces to a set of second-order differential equations given by

$$-\frac{U''_{nl'}(r)}{2} - \frac{\alpha e^{-\alpha r}}{1-e^{-\alpha r}} + \frac{1}{2}\frac{\lambda}{r^2}U_{nl'}(r) = EU_{nl'}(r), \quad (6)$$

$$-\frac{1}{\sin\theta}\frac{d}{d\theta}\left(\sin\theta\frac{d}{d\theta}\right)\Theta_{l'm}(\theta) + \frac{m^2}{\sin^2\theta}\Theta_{l'm}(\theta) + 2\beta\frac{\cos^2\theta}{\sin^2\theta}\Theta_{l'm}(\theta) = \lambda\Theta_{l'm}(\theta) \quad (7)$$

and

$$\frac{d^2\Phi_m(\phi)}{d\phi^2} + m^2\Phi_m(\phi) = 0, \quad (8)$$

where λ and m are the separation constants. The boundary conditions for equation (7) require that both $\Theta(0)$ and $\Theta(\pi)$ must take finite values. In the general solution of spherically symmetric potentials, λ is $l(l+1)$. The nomenclature of the energy states is retained as in the spherically symmetric potential in order to make a clear representation. As there is azimuthal symmetry in the present problem, the azimuth part

of the wave function Ψ in equation (8) has the general solution

$$\Phi_m(\phi) = \frac{1}{\sqrt{2\pi}} \exp(\pm i m\phi), \tag{9}$$

where m is the usual magnetic quantum number. In the present case we take $m = 0$ and solve equations (6) and (7) by finite difference method to get the energy spectrum as well as the corresponding wave functions. The 2^l-pole radial matrix elements can easily be calculated using these wave functions.

The exact analytical solution of equations (6) and (7) for coulomb-type potential $-Z/r$ combined with the ring-potential has been given by Chen and Dong [31] for bound states as well as continuous states. The solution for bound states is given as

$$E = -\frac{Z^2}{2(n_r + L + 1)^2} = -\frac{Z^2}{2(n')^2}, \tag{10}$$

where

$$n' = n_r + L + 1 = \frac{1}{2}[2n_r + \sqrt{1 + 4[(k + \sqrt{2\beta + m^2})(k + \sqrt{2\beta + m^2} + 1) - 2\beta]} + 1] \tag{11}$$

and $|m|$, k, $n_r = 0, 1, 2, \ldots$. n_r is the number of nodes of the corresponding radial wave functions. For details, please see [31]. This expression has been quoted here as the results calculated in the present case for some of the bound states have been matched with the analytical solution for energy levels given by equation (10) and a good agreement has been found.

The dimensionless physical quantity called oscillator strength which signifies the strength of transitions due to interaction of confined particle with electromagnetic radiation represents the intensity of spectral lines, thus playing a very important role in the study of the optical properties related to the electronic transitions [53, 54]. The 2^l-pole oscillator strengths for transitions from an initial state n to a final state n', corresponding to absorption or emission of photons, is given by the standard formula [55–57]

$$f^{(l)}_{n\to n'} = 2|\langle \Psi_n(r)|r^l \cos^l\theta|\Psi_{n'}(\vec{r})\rangle|^2 (E_{n'} - E_n), \tag{12}$$

where $l = 1, 2, 3$ for dipole, quadrupole and octupole cases, respectively.

Another important microscopic quantity that can be determined using the data of oscillator strengths is the polarizability [58, 59], the knowledge of which has applications in many areas of chemistry and physics like optics, chemical structure and interaction of molecules with light. The polarizabilities are also helpful in understanding the physical, electronic, and optical properties of particles. For example, it is related to another experimentally significant macroscopic property called refractive index [60]. The static 2^l-pole polarizability in terms of oscillator strengths for different energy state combinations is given by the relation [55–57, 61]

$$\alpha_l = \sum_{n'\neq n} \frac{f^{(l)}_{n\to n'}}{(E_{n'} - E_n)^2}, \tag{13}$$

where the summation is over all intermediate states including the continuum.

One of the interesting physical properties which can be deduced from the present results is the diamagnetic screening constant. The electrons near the nucleus affect the value of applied magnetic field. This causes screening effect which is described by the screening constant and is responsible for a slight change in Larmor frequency resulting in chemical shift. The position and number of chemical shifts are useful tools for determining the structure of a molecule. An average value of the screening constant for a molecule can be determined in high-resolution solution NMR. The diamagnetic and paramagnetic components of this constant are related to the orbital motion of the electrons and other significant properties of the molecule, respectively. For hydrogen atom, the diamagnetic component dominates and has a relatively smaller chemical shift range in comparison to heavier atoms [62]. This constant is defined as [63]

$$\sigma = \frac{e^2}{3m_e c^2} \langle \psi_{1s}| \frac{1}{r} |\psi_{1s}\rangle. \tag{14}$$

3. Results and discussions

A particle confined in Hulthén plus ring-shaped potential given by equation (2) has been considered. In order to get the energy spectrum for particular values of confinement parameters α and β, equation (7) is first solved which gives the angular part of the solution λ which is then used in equation (6) to get the complete solution. Both these equations have been solved in MATLAB by employing the finite difference approach. The energy spectra consists of both negative and positive-energy states. The negative-energy states are considered to be bound states while positive-energy states are taken as unbound ionized states forming a pseudocontinuum. The wave function corresponding to each energy level is also obtained which makes the calculation of radial matrix elements for different combinations of energy states possible. λ which has a value l $(l + 1)$ for spherically symmetric potentials, is significantly altered by β, as mentioned in section 2 This effect on the first eight values of the parameter λ, which correspond to the first eight values of orbital angular momentum, has been shown in figure 1. On the basis of the observed increase in λ with β, it can be easily predicted that the ring potential would strongly affect all the properties to be studied in the present problem.

Hulthén potential has been studied vastly in the literature due to its importance in a number of subjects of interest. The main aim of the present paper is to investigate the role of ring potential on various properties of the system. $\beta = 0$ refers to the case of pure spherically symmetric Hulthén potential. Therefore, the results corresponding to $\beta = 0$ have been calculated and included for all the properties that have been considered. These results can serve as a ready reference for analyzing the effect of β. Figure 2 shows the variation of first ten energy levels with respect to α, i.e. the confinement

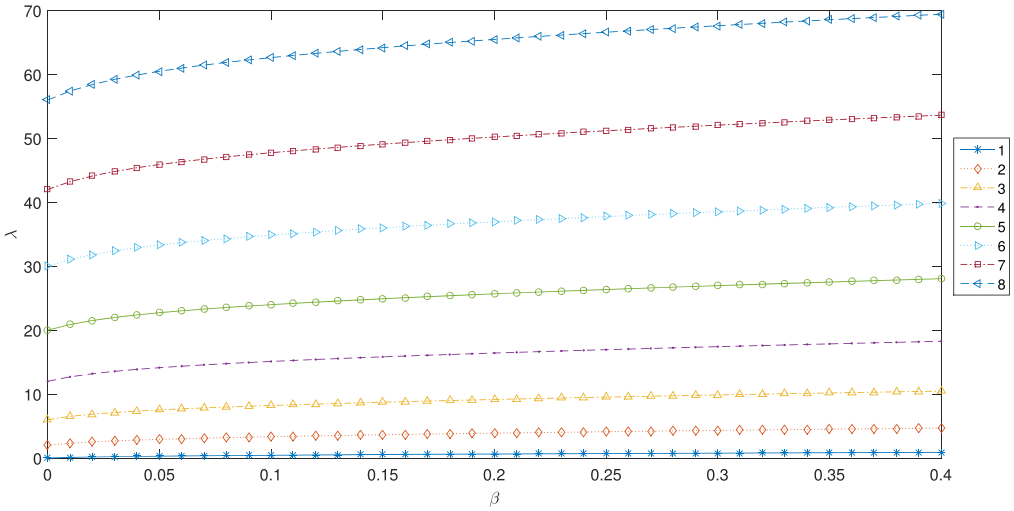

Figure 1. Variation of first eight values of λ with β.

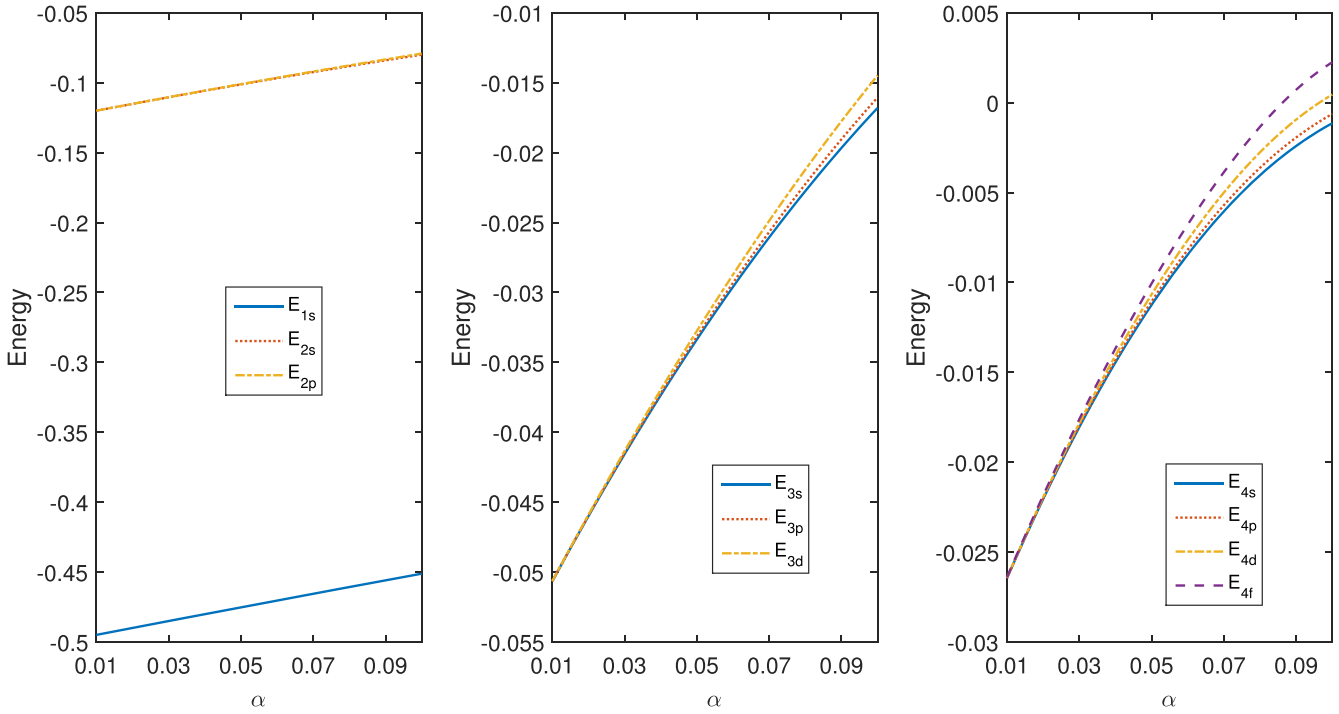

Figure 2. Variation of first ten energy levels with α for $\beta = 0$ a.u.

parameter related to the Hulthén potential, with α ranging from 0.01 to 0.1 for $\beta = 0$. The break in degeneracy as well as the increase in the energy value due to increase in α as observed in the present case is a well-known feature of confinement related to spherically symmetric Hulthén potentials [64–67] or radial confinement, in general [68]. It can be seen from figure 2 that for higher values of α, 4*d* and 4*f* states become positive or unbound and hence form a part of the pseudocontinuum. The number of bound states are hence found to decrease as an effect of confinement, as expected. In figure 3, the variation of first ten energy levels with respect to α for $\beta = 0.4$ is shown. Due to the presence of the ring potential, i.e. finite β, degeneracy has been lifted for smaller values of α too.

Figures 4 and 5 show the variation of first ten energy levels with β for $\alpha = 0.01$ and 0.1, respectively. Effects of confinement similar to those interpreted from figures 2 and 3 for α are true for β also with the maximum effects seen for high α and β in figure 5 for the states with principal quantum number $n = 4$. Since α represents screening which is expected to be more for states which are higher in energy and also maximum effect of confinement is expected on states which are at large distances from the nuclei, the observed variation of energy levels with α and β is obvious.

As a check on our results some of the energy levels for pure Hulthén case, i.e. for $\beta = 0$, have been compared with the results presented by Varshni [7] and many others in table 1 and quite a good agreement has been found. As the

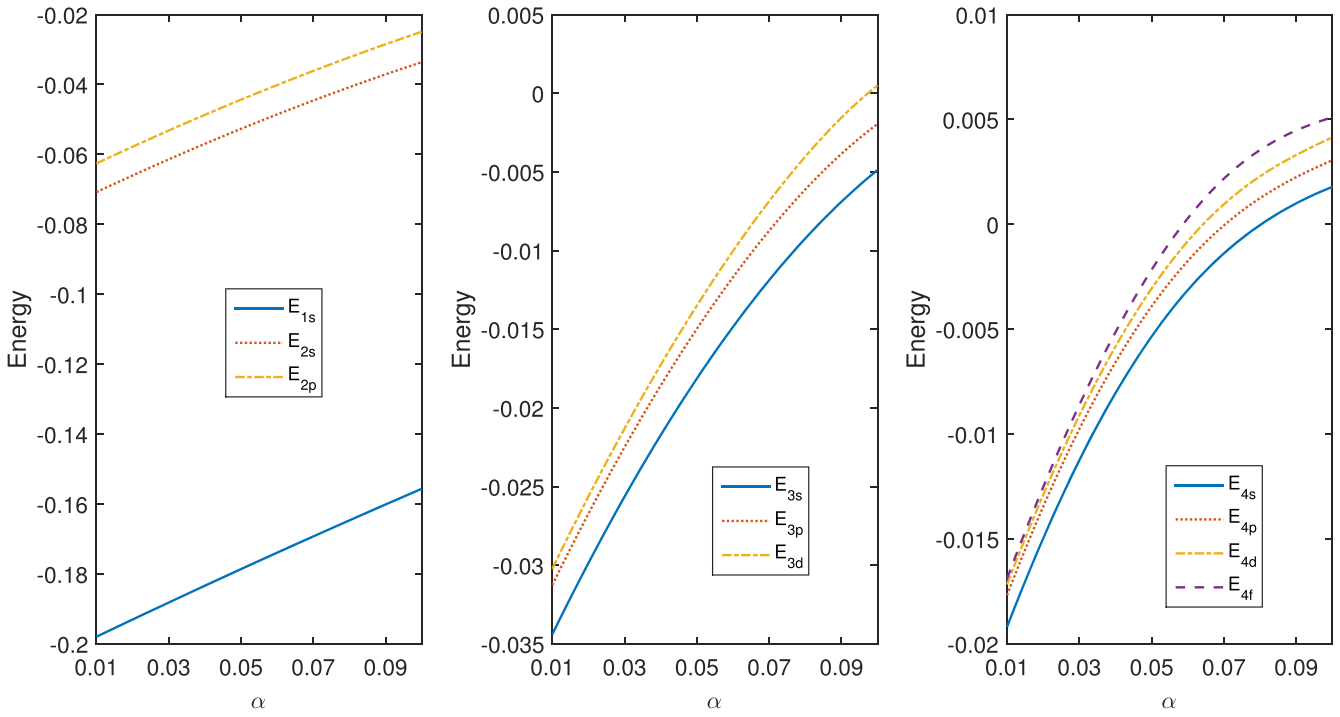

Figure 3. Same as figure 2 for $\beta = 0.4$ a.u.

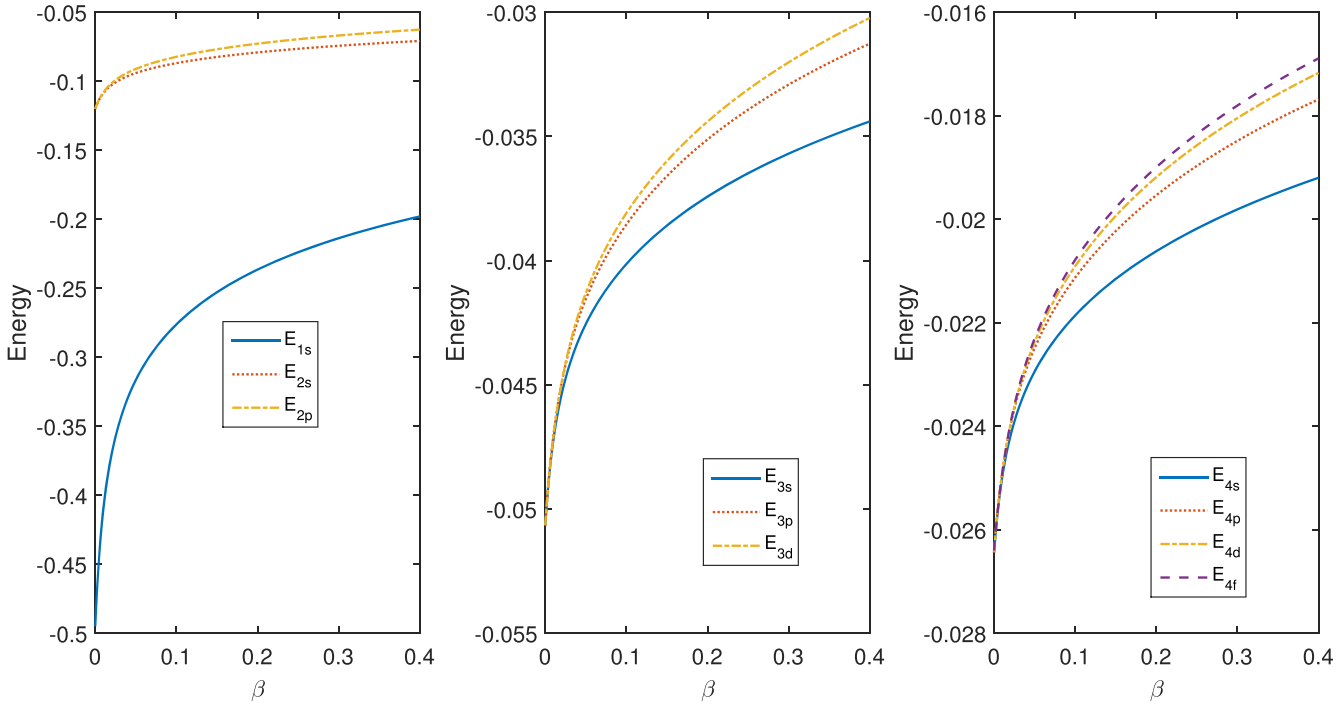

Figure 4. Variation of first ten energy levels with β for $\alpha = 0.01$ a.u.

Hulthén potential reduces to Coulomb form for small values of α, the potential in equation (2) is then similar to that considered by Chen and Dong [31]. Also, in the limiting case of very small α and β, the present problem reduces to the case of a particle in inverse square potential which is another interesting case. In order to check the calculations for angular part of Schrödinger equation, the first ten energy levels for a particular value of $\beta(= 0.2)$ have been compared with those calculated using the analytical expression for exact solutions of the bound states given by Chen and Dong [31] as given by equation (10) by taking very small value of α, viz., 0.0001. Also the energy levels have been calculated by taking Coulomb potential instead of Hulthén in the Schrödinger equation. For both these cases the results have been presented in table 2 which authenticates our calculations.

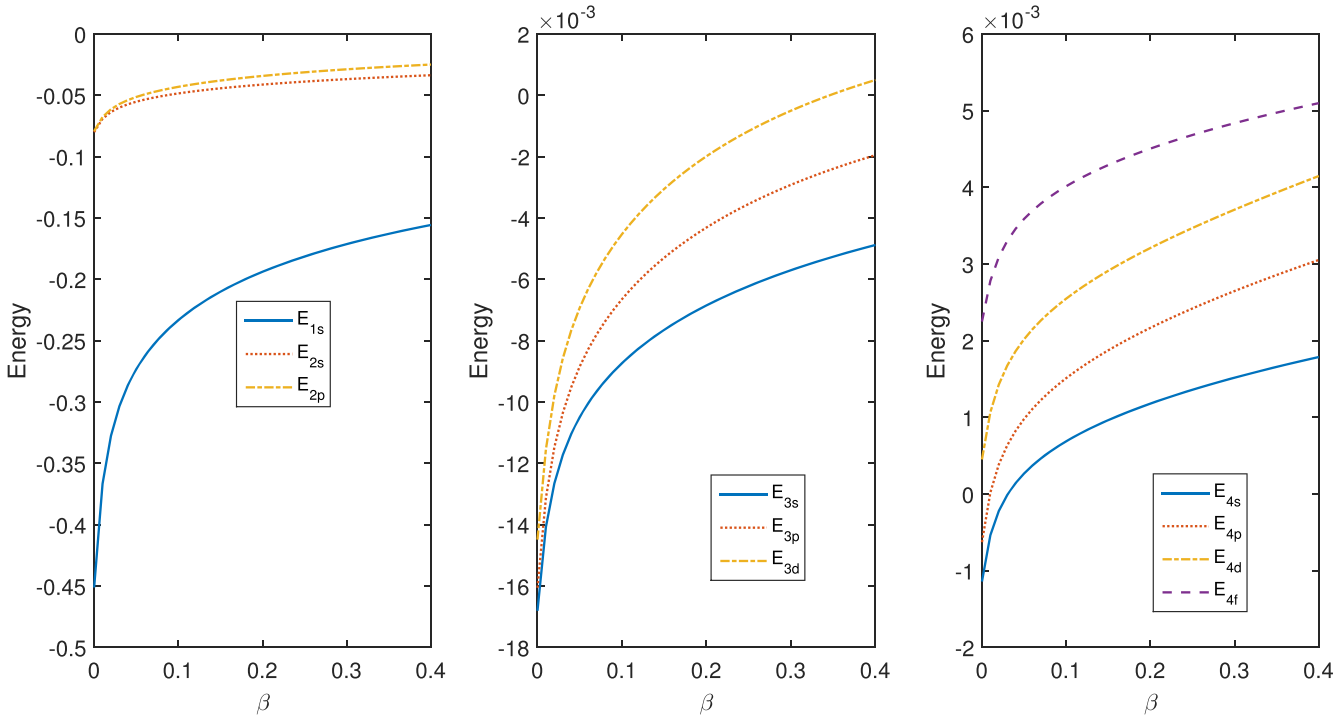

Figure 5. Same as figure 4 for $\alpha = 0.1$ a.u.

Table 1. Comparison of energy levels for pure Hulthén potential ($\beta = 0$) with ([7] and references therein). Atomic units are used.

	E_{2p}		E_{3p}		E_{3d}	
α	Present	Reference [7]	Present	Reference [7]	Present	Reference [7]
0.025	−0.112 76	−0.112 76	−0.043 71	−0.043 71	−0.043 60	−0.043 60
0.05	−0.101 05	−0.101 04	−0.033 17	−0.033 16	−0.032 75	−0.032 75
0.075	−0.089 85	−0.089 84	−0.023 94	−0.023 94	−0.023 03	−0.023 03
0.1	−0.079 18	−0.079 18	−0.016 05	−0.016 05	−0.014 48	−0.014 48
0.150	−0.059 44	−0.059 44	−0.004 47	−0.004 47	−0.001 39	−0.001 40
0.2	−0.041 89	−0.041 89	0.000 91		0.003 04	
0.250	−0.026 61	−0.026 61	0.001 86		0.003 30	
0.3	−0.013 79	−0.013 79	0.002 06		0.003 36	
0.350	−0.003 79	−0.003 79	0.002 20		0.003 38	

The validity of comparison theorem of Quantum Mechanics [69] for four different potentials, viz., Coulomb, Hulthén, Yukawa and Hulthén2 where Hulthén2 is of the same form as Hulthén but with α taken to be twice of α for Hulthén, has been investigated. This theorem predicts that if the potentials V_a and V_b are ordered such that $V_a < V_b$, then the corresponding energy eigenvalues are also ordered, that is, $E_a < E_b$. Since the four central potentials are ordered such that $V_{\text{Coulomb}} < V_{\text{Hulthen}} < V_{\text{Yukawa}} < V_{\text{Hulthen2}}$, the energy spectra is similarly ordered. This ordering is not expected to depend on the sphericity or ring potential. This fact has been shown to be valid by comparing energy eigenvalues for different values of α and β in table 3.

The 2^l-pole radial matrix elements for $l = 1, 2, 3$ have been calculated for different values of α and β. The data has been plotted in figures 6–9 for some particular combinations of energy states, viz., $\langle 1s|r^l|2s\rangle$, $\langle 1s|r^l|2p\rangle$, $\langle 1s|r^l|3s\rangle$, $\langle 1s|r^l|3p\rangle$, $\langle 1s|r^l|3d\rangle$, $\langle 2s|r^l|2p\rangle$, $\langle 3p|r^l|3d\rangle$ and $\langle 4d|r^l|4f\rangle$. The variation of the dipole ($l = 1$), quadrupole ($l = 2$) and octupole ($l = 3$) matrix elements with α has been shown in figure 6 for $\beta = 0$ and in figure 7 for $\beta = 0.4$. Their variation with respect to β

Table 2. Comparison of energy levels for $\alpha = 0.0001$ and $\beta = 0.2$ and Coulomb potential with [31]. Atomic units are used.

Energy level	Present ($\alpha = 0.0001$)	Present (Coulomb potential)	Reference [31]
1*s*	−0.241 41	−0.241 46	−0.241 33
2*s*	−0.084 00	−0.084 05	−0.084 02
2*p*	−0.077 67	−0.077 72	−0.077 71
3*s*	−0.042 23	−0.042 28	−0.042 27
3*p*	−0.039 93	−0.039 98	−0.039 98
3*d*	−0.039 23	−0.039 28	−0.039 28
4*s*	−0.025 32	−0.025 37	−0.025 37
4*p*	−0.024 24	−0.024 29	−0.024 30
4*d*	−0.023 91	−0.023 96	−0.023 96
4*f*	−0.023 75	−0.023 80	−0.023 80

Table 3. Validity of comparison theorem in presence of β. Atomic units are used.

Potential	1*s*	2*s*	2*p*	3*s*	3*p*	3*d*	4*s*	4*p*	4*d*	4*f*
$\alpha = 0.01$	$\beta = 0$									
Coulomb	−0.499 87	−0.124 99	−0.125 00	−0.055 55	−0.055 56	−0.055 56	−0.031 25	−0.031 25	−0.031 25	−0.031 25
Hulthén	−0.494 89	−0.120 04	−0.120 04	−0.050 67	−0.050 66	−0.050 64	−0.026 45	−0.026 44	−0.026 43	−0.026 40
Yukawa	−0.489 95	−0.115 29	−0.115 25	−0.046 20	−0.046 15	−0.046 06	−0.022 36	−0.022 31	−0.022 23	−0.022 10
Hulthén2	−0.489 92	−0.115 19	−0.115 17	−0.046 00	−0.045 97	−0.045 91	−0.022 05	−0.022 02	−0.021 95	−0.021 85
$\alpha = 0.01$	$\beta = 0.4$									
Coulomb	−0.202 94	−0.075 72	−0.067 53	−0.039 24	−0.036 11	−0.035 10	−0.023 94	−0.022 43	−0.021 93	−0.021 68
Hulthén	−0.197 97	−0.070 80	−0.062 60	−0.034 40	−0.031 26	−0.030 23	−0.019 20	−0.017 68	−0.017 17	−0.016 89
Yukawa	−0.193 10	−0.066 18	−0.057 95	−0.030 12	−0.026 97	−0.025 86	−0.015 33	−0.013 83	−0.013 25	−0.012 86
Hulthén2	−0.193 05	−0.066 04	−0.057 82	−0.029 86	−0.026 73	−0.025 64	−0.014 97	−0.013 46	−0.012 90	−0.012 53
$\alpha = 0.1$	$\beta = 0$									
Coulomb	−0.499 87	−0.124 99	−0.125 00	−0.055 55	−0.055 56	−0.055 56	−0.031 25	−0.031 25	−0.031 25	−0.031 25
Hulthén	−0.451 12	−0.079 99	−0.079 18	−0.016 80	−0.016 05	−0.014 48	−0.001 14	−0.000 63	0.000 45	0.002 25
Yukawa	−0.406 93	−0.049 92	−0.046 54	−0.003 20	−0.001 58	0.001 62	0.002 10	0.002 69	0.004 05	0.004 58
Hulthén2	−0.404 87	−0.044 99	−0.041 89	−0.000 49	0.000 91	0.003 04	0.002 95	0.003 75	0.006 14	0.004 90
$\alpha = 0.1$	$\beta = 0.4$									
Coulomb	−0.202 94	−0.075 72	−0.067 53	−0.039 24	−0.036 11	−0.035 10	−0.023 94	−0.022 43	−0.021 93	−0.021 68
Hulthén	−0.155 65	−0.033 63	−0.024 93	−0.004 88	−0.001 95	0.000 50	0.001 79	0.003 05	0.004 15	0.005 10
Yukawa	−0.117 49	−0.012 26	−0.003 34	0.001 05	0.002 65	0.004 13	0.005 21	0.007 22	0.008 68	0.006 17
Hulthén2	−0.113 81	−0.007 62	0.000 91	0.001 80	0.003 36	0.004 50	0.006 33	0.008 46	0.009 78	0.006 40

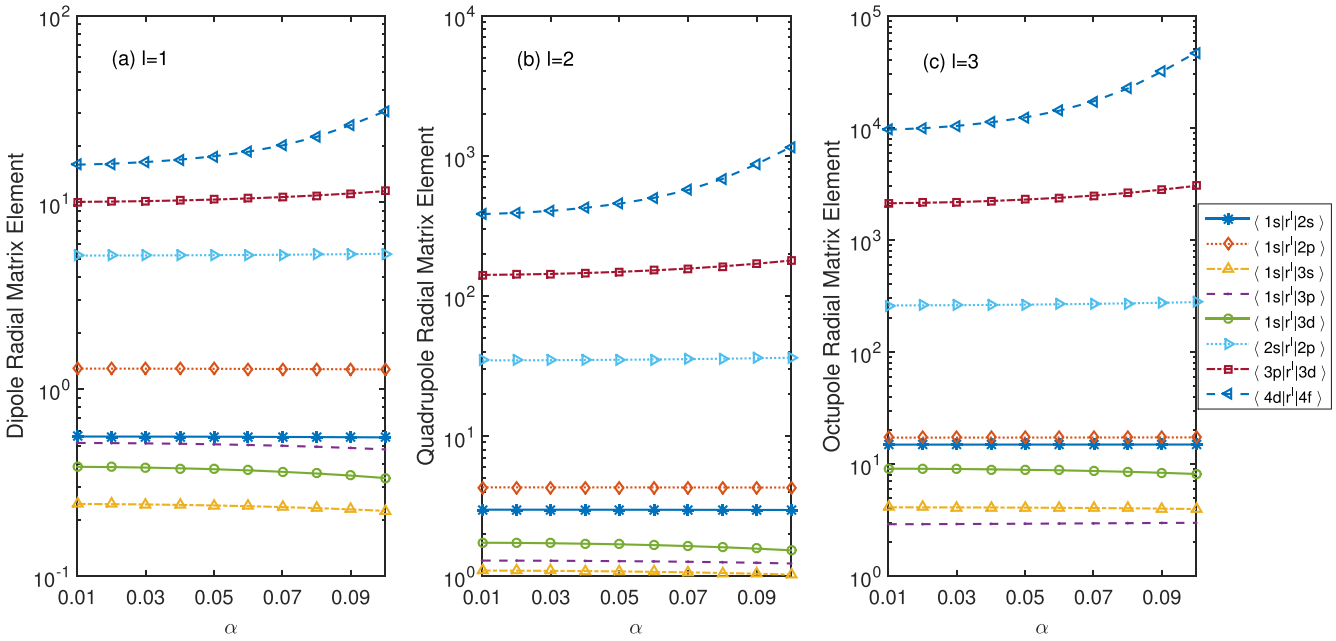

Figure 6. Variation of 2^l-pole radial matrix elements with α for $\beta = 0$ a.u. (a) $l = 1$ (b) $l = 2$ (c) $l = 3$.

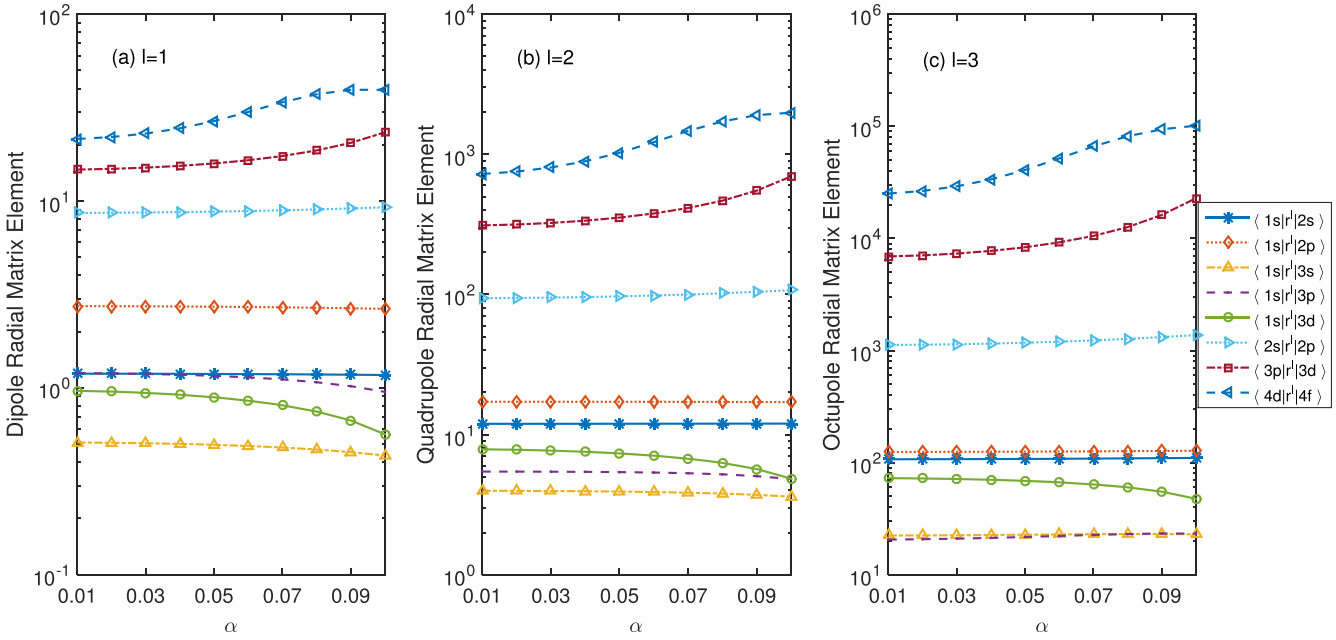

Figure 7. Same as figure 6 for $\beta = 0.4$ a.u.

has been shown in figures 8 and 9 for $\alpha = 0.001$ and 0.1, respectively. Semilog scale has been employed to plot figures 6–9 to make the variation more apparent. This study of radial matrix elements is important as it is the starting point of obtaining many properties of great significance, e.g. oscillator strengths and polarizabilities which are a part of the problem under study. The radial matrix elements, in general, are more for octupole than quadrupole which, in turn, are greater than those for dipole interactions.

The radial matrix elements along with the angular contributions calculated using the wave functions given by the solution of equation (7) are employed to calculate important optical properties, viz., oscillator strengths and static polarizabilities. In order to provide a glimpse of the effect of the parameter β, characterizing the ring potential, on the angular part of dipole matrix elements, $\langle\gamma_\lambda|\cos\theta|\gamma_{\lambda'}\rangle$, the variation of these matrix elements with β for some combinations of l and l' has been shown in table 4. The magnetic quantum number m has been taken to be zero. These matrix elements provide a measure of the non-sphericity of the system. A significant decrease in these matrix elements with increase in β evident from table 4 indicates the effect of the ring potential. An interesting observation is that as we switch to the dipole elements between higher energy levels the decrease in the

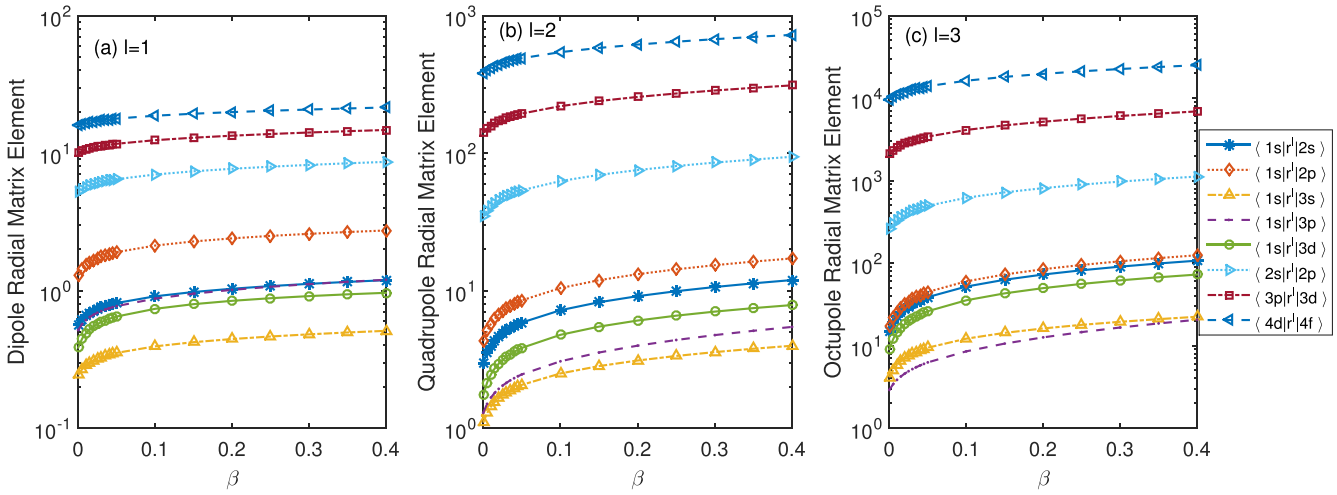

Figure 8. Variation of 2^l-pole radial matrix elements with β for $\alpha = 0.01$ a.u. (a) $l = 1$ (b) $l = 2$ (c) $l = 3$.

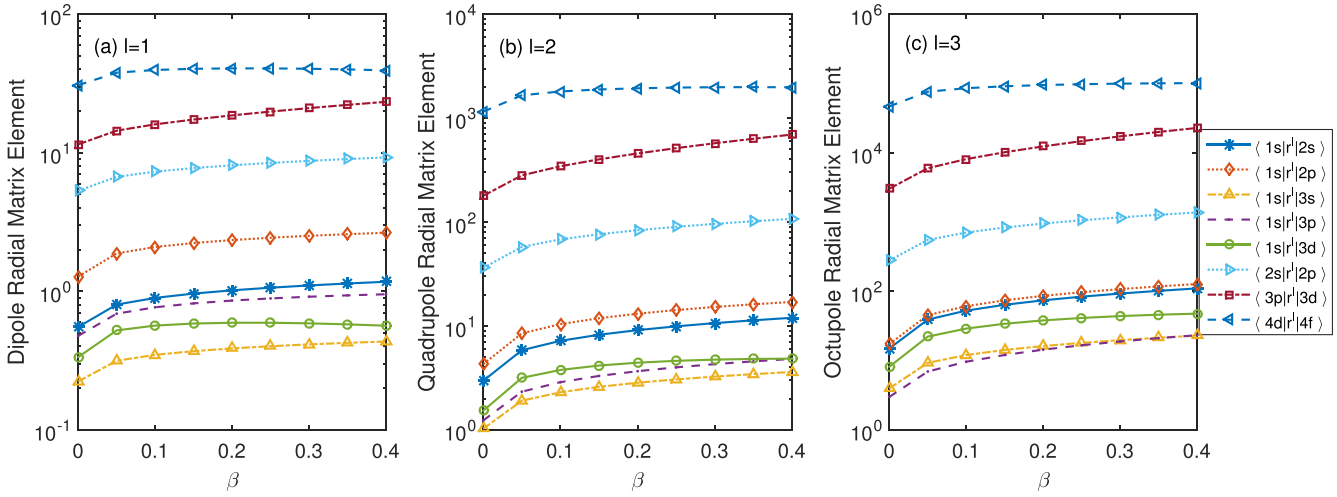

Figure 9. Same as figure 8 for $\alpha = 0.1$ a.u.

matrix elements with increase in β reduces. Also, for $\beta = 0$ and 0.1 the matrix elements corresponding to higher states decrease but the trend is opposite for $\beta = 0.2$–0.4. This may be an indication of very strong non- sphericity introduced in the system by the ring potential. Since the matrix elements play a crucial role in determination of oscillator strengths and polarizabilities, the presence of ring potential is expected to alter the dynamics of the system to a great extent.

The dipole, quadrupole and octupole oscillator strengths have been evaluated using equation (12) for various values of α and β. The validity of *f*-sum rule has been ensured for dipole oscillator strengths both for low as well as high α and β, which again verifies our calculations. The variation of dipole, quadrupole and octupole oscillator strengths with α have been shown in figures 10 and 11 for $\beta = 0$ and 0.4, respectively. In figures 12 and 13, the variation has been shown with respect to β for $\alpha = 0.01$ and 0.1, respectively. Semilog scale has been used in part (c) of figures 10–13 for octupole oscillator strengths and also in figures 10 and 12 for dipole oscillator strengths to make the variation more apparent.

Table 4. Variation of angular part of dipole matrix elements with β for some combinations of λ and λ'. The corresponding values of l and l' for the spherically symmetric case as mentioned in columns 1 and 2 serve as reference index for rest of the β values. Atomic units are used.

		$\langle\gamma_\lambda\lvert\cos\theta\rvert\gamma_{\lambda'}\rangle$				
l	l'	$\beta = 0$	$\beta = 0.1$	$\beta = 0.2$	$\beta = 0.3$	$\beta = 0.4$
0	1	0.577 35	0.506 99	0.484 25	0.468 85	0.456 97
1	2	0.516 40	0.502 36	0.494 38	0.488 12	0.482 79
2	3	0.507 09	0.501 24	0.497 12	0.493 71	0.490 70
3	4	0.503 95	0.500 79	0.498 25	0.496 11	0.494 17
4	5	0.502 52	0.500 57	0.498 83	0.497 35	0.496 00
5	6	0.501 75	0.500 45	0.499 17	0.498 09	0.497 09

In order to check our results, the dipole oscillator strengths calculated for pure Hulthén case, i.e. for $\beta = 0$, have been matched with those given by Varshni [7] and Bahar *et al* [10] and the values have been found to be in close agreement. The comparison has been shown in table 5. It may be mentioned that although the solution of the angular part of

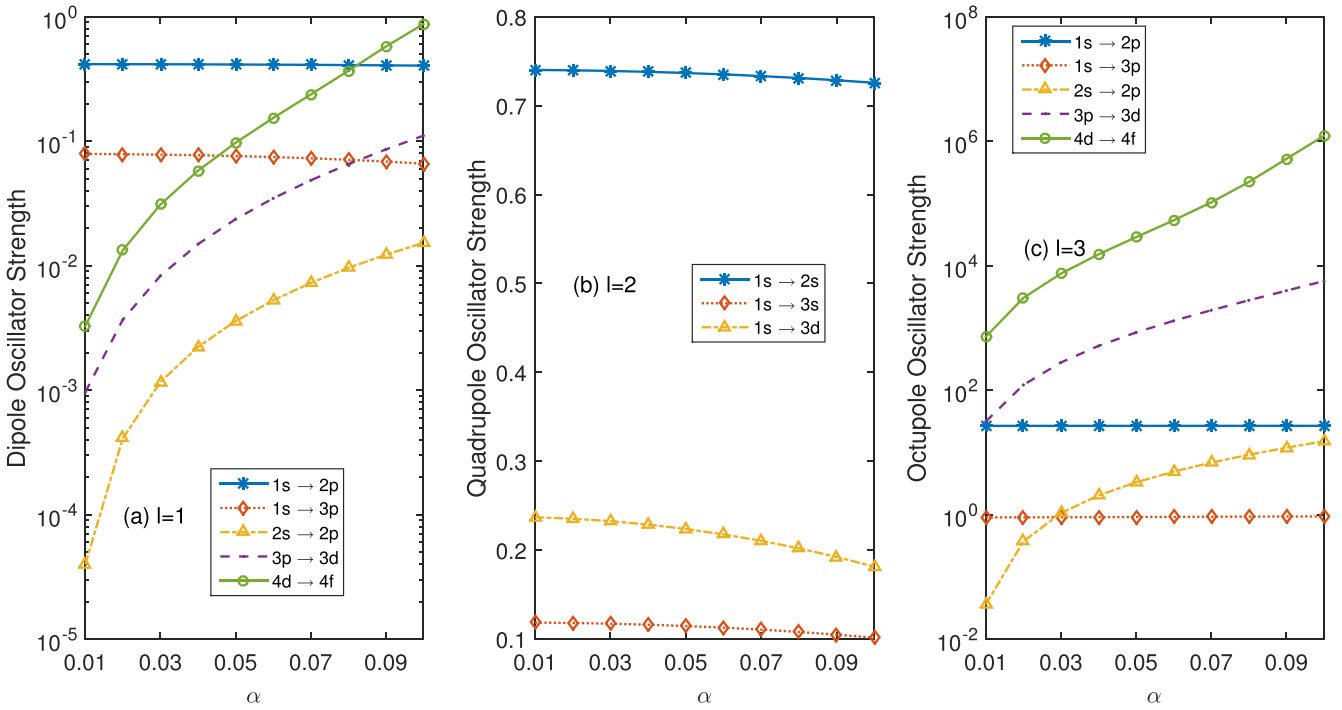

Figure 10. Variation of 2^l-pole oscillator strengths with α for $\beta = 0$ a.u. (a) $l = 1$ (b) $l = 2$ (c) $l = 3$.

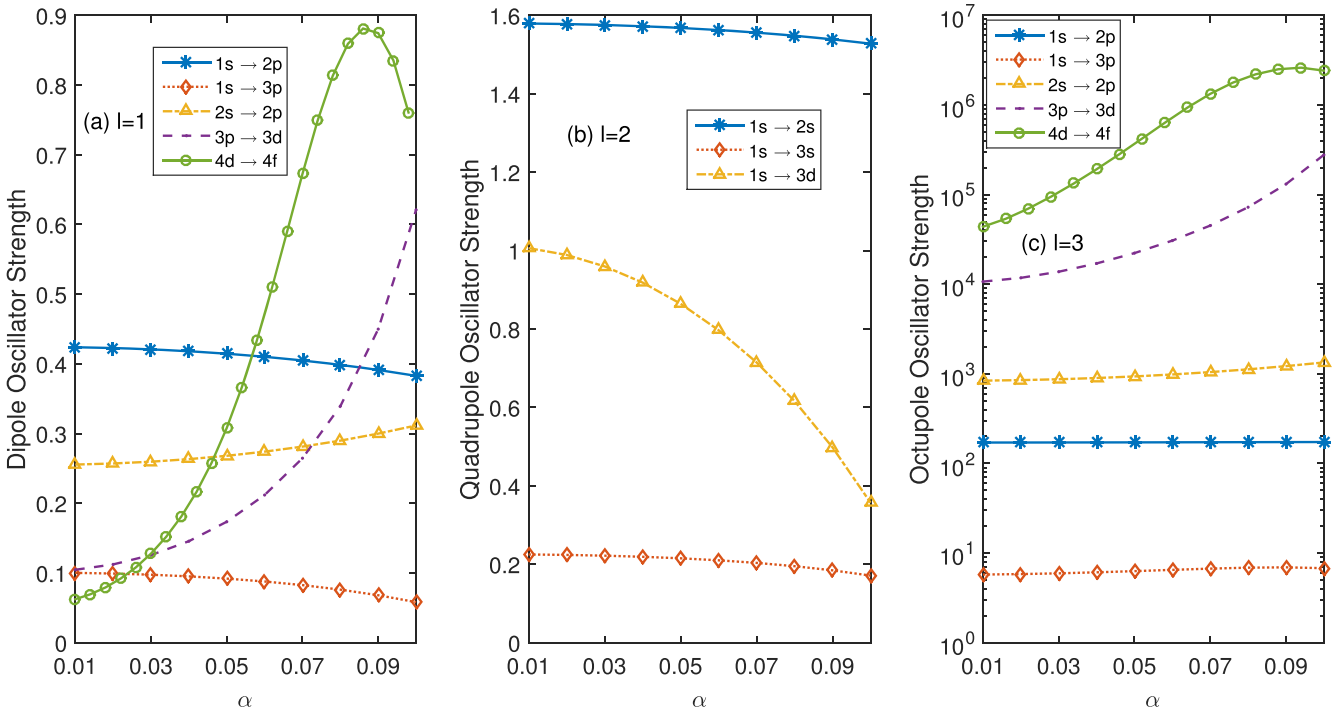

Figure 11. Same as figure 10 for $\beta = 0.4$ a.u.

the Schrödinger equation for the present problem does not give an integral value for orbital angular momentum l, the oscillator strengths that have been calculated are found to follow the selection rules as is valid for dipole, quadrupole or octupole allowed transitions. Out of the set of combinations of energy levels for which matrix elements have been plotted in figures 6–9, only the oscillator strengths which have finite values have been plotted in figures 10–13.

Oscillator strengths being product of matrix elements and the difference of corresponding energy levels, are found to either increase or decrease depending on the variation of these quantities. For example, in figure 10 dipole oscillator strength for $1s \rightarrow 2p$ is found to decrease very slightly with α but for $4d \rightarrow 4f$ it increases prominently. This can be easily inferred from the variation of corresponding energy difference in figure 2 and radial matrix elements in figure 6. Since the finite

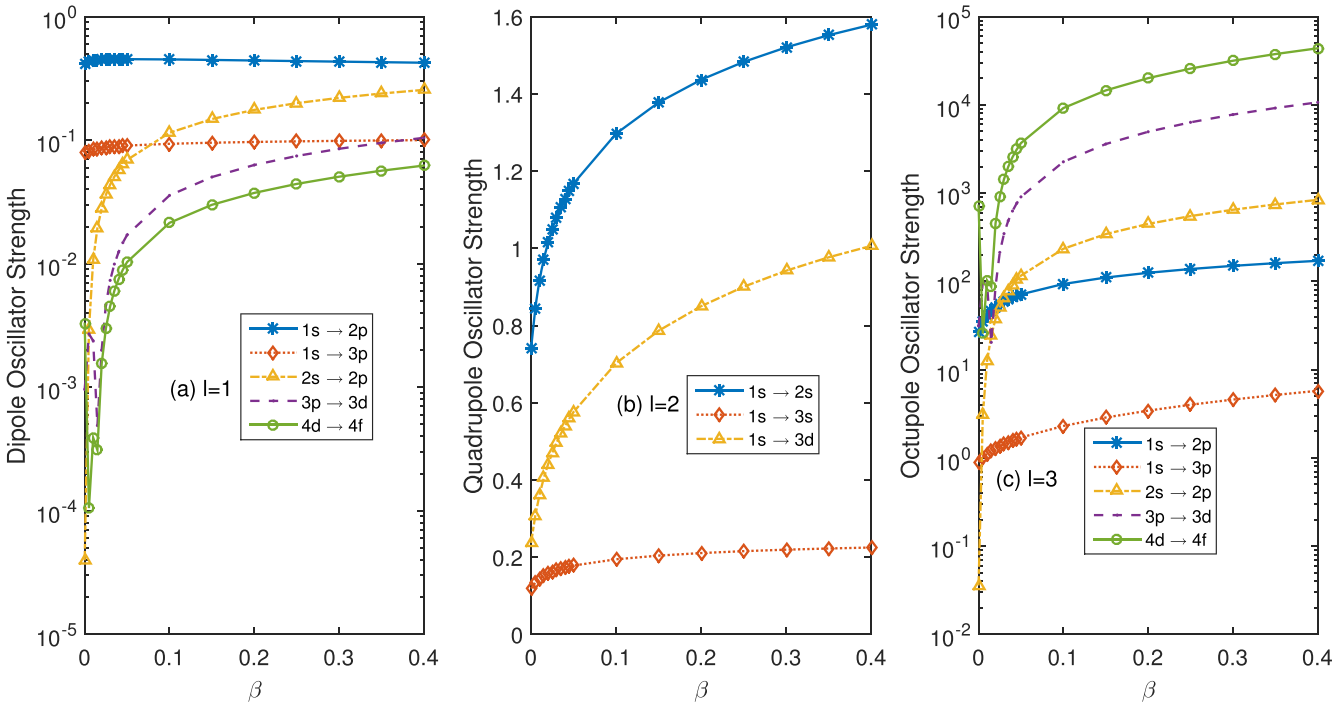

Figure 12. Variation of 2^l-pole oscillator strengths with β for $\alpha = 0.01$ a.u. (a) $l = 1$ (b) $l = 2$ (c) $l = 3$.

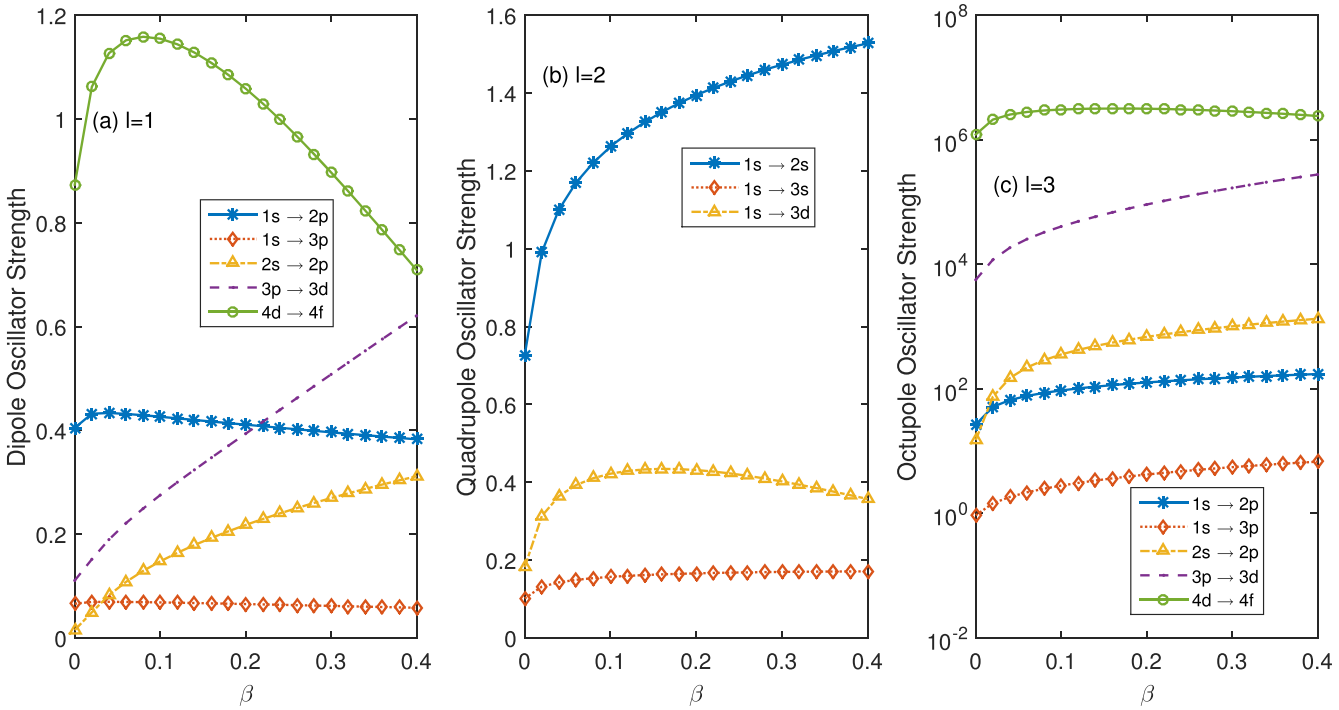

Figure 13. Same as figure 12 for $\alpha = 0.1$ a.u.

value of β in figure 11 changes only the angular part of the matrix elements, which is not affected by a change in α, the patterns of variation of oscillator strengths in figure 11 can, therefore, be explained on the basis of variation of corresponding energy difference and radial matrix elements. The dependence of oscillator strengths on β in figures 12 and 13 can be interpreted in an analogous manner by taking into account the angular contribution to matrix elements. In general, since oscillator strength expresses the probability of absorption or emission of electromagnetic radiation for quantum transitions between energy levels of the system, the data analysis presented for oscillator strengths would be useful for studying atomic interaction with such radiation.

Static dipole, quadrupole and octupole polarizabilities, taking 1s ground state as the initial state, have been evaluated for various values of α and β using equation (13). The

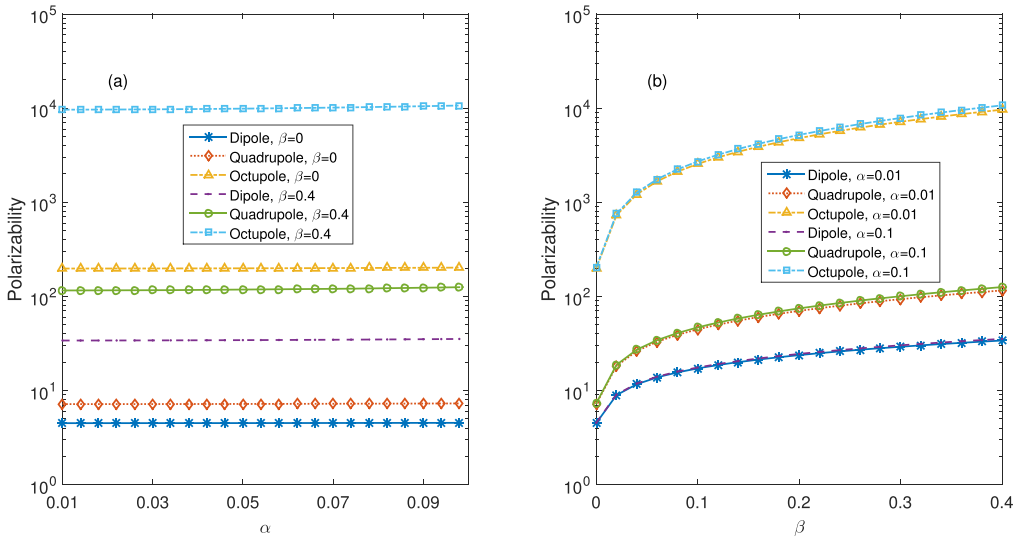

Figure 14. Variation of polarizabilities (a) with α for $\beta = 0$ and 0.4 a.u. and (b) with β for $\alpha = 0.01$ and 0.1 a.u.

Table 5. Comparison of dipole oscillator strengths for pure Hulthén potential ($\beta = 0$). Atomic units are used.

α	$1s \rightarrow 2p$			$1s \rightarrow 3p$		
	Present	Reference [7]	Reference [10]	Present	Reference [7]	Reference [10]
0.025	0.415 64	0.415 50	0.415 40	0.078 34	0.078 34	0.078 30
0.05	0.413 52	0.413 40	0.413 10	0.076 00	0.076 00	0.075 90
0.075	0.409 96	0.409 80	0.409 30	0.071 96	0.071 96	0.071 90
0.1	0.404 89	0.404 70	0.403 90	0.065 98	0.066 00	0.066 00
0.15	0.389 87	0.389 70	0.388 20	0.046 26	0.046 33	0.047 80
0.2	0.367 36	0.367 10	0.365 50	0.013 20		
0.25	0.335 30	0.334 80	0.334 90	0.002 78		
0.3	0.289 62	0.288 60	0.295 40	0.002 23		
0.35	0.218 61	0.216 90	0.245 10	0.005 94		

polarizabilities have been plotted with respect to α in figure 14(a) for $\beta = 0$ and 0.4 and in figure 14(b) with respect to β for $\alpha = 0.01$ and 0.1, respectively. The figure has been plotted in semilog scale in order to make a comprehensible comparative presentation. A comparison of dipole polarizability calculated for pure Hulthén potential, i.e. $\beta = 0$, with the values calculated by Bahar *et al* [10] has been presented in table 6. The values are found to follow an increasing trend with increase in α in consonance with the data of [10] presented in the table.

Figure 14 shows that the polarizabilities rapidly increase with β as compared to that with α and this change is fast for lower values of β. The dipole and quadrupole polarizabilities have been found to increase only slightly with increase in α for $\beta = 0$ as seen from figure 14(a). On the other hand, the octupole polarizability increases appreciably. The trend is same for $\beta = 0.4$ but is comparatively more prominent. It can be observed from figure 14(b) that the increase is more for quadrupole polarizability than for the dipole polarizability and much more for octupole polarizability. For $\alpha = 0.1$, the polarizabilites increase to a value greater than that for $\alpha = 0.01$. The increase in the value of polarizabilites with increase in the screening parameter α means that the stronger screening effect of the Hulthén potential leads to easier polarization of the atoms. The much larger increase with β depicts very strong dependence on the ring potential.

Table 6. Comparison of dipole polarizability for pure Hulthén potential ($\beta = 0$). Atomic units are used.

α	Present	Reference [10]
0.01	4.503 65	4.500 37
0.015	4.504 11	4.500 84
0.02	4.504 77	4.501 49
0.025	4.505 61	4.502 33
0.03	4.506 64	4.503 36
0.04	4.509 25	4.505 97
0.05	4.512 62	4.509 34
0.06	4.516 74	4.513 45
0.07	4.521 62	4.518 33
0.09	4.533 66	4.530 35
0.1	4.540 84	4.537 52
0.2	4.656 31	4.652 84

The diamagnetic screening constant defined by equation (14) has also been calculated and its variation with β for three different values of α has been represented in

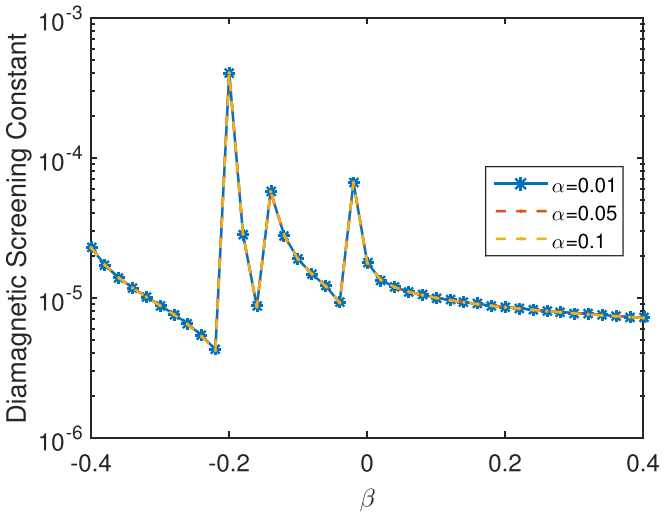

Figure 15. Variation of diamagnetic screening constant with β for $\alpha = 0.01$, $\alpha = 0.05$ and 0.1 a.u.

figure 15. As can be seen from the figure, the parameter α hardly influences the screening constant but change in β has a much greater effect on it. The reason for this kind of variation is that the ground state wavefunction does not change much with α in the range considered but a slight change in β significantly alters it.

4. Conclusions

The energy spectrum and wave functions of a particle confined in Hulthén plus ring-shaped potential have been evaluated numerically by employing finite difference method to solve the corresponding Schrödinger equation. The effect of the confinement parameters of both these potentials has been studied on the energy spectrum, 2^l-pole radial matrix elements for $l = 1, 2, 3$ as well as on important optical properties, viz., dipole, quadrupole and octupole oscillator strengths and static polarizabilities. The non-sphericity introduced due to the presence of ring potential has been found to significantly change the angular part of matrix elements which in turn would have a considerable impact on dynamics of the system subjected to external fields. Also, the validity of the comparison theorem of Quantum Mechanics for energy eigenvalues for four different potentials, viz., Coulomb, Hulthén, Yukawa and Hulthén2 is found to be independent of the presence of ring potential.

Acknowledgments

One of us (VP) is thankful to UAM Iztapalapa for hospitality during the course of this work and also KDS is thankful to Indian National Science Academy, New Delhi, for support under its senior scientist program.

Contribution of authors

All authors contributed equally to the paper.

Declarations of interest

None.

ORCID iDs

Sonia Lumb https://orcid.org/0000-0001-6715-407X
Vinod Prasad https://orcid.org/0000-0002-0154-3221

References

[1] Hulthén L 1942 *Ark. Mat. Astron. Fys.* A **28A** 5
[2] Flügge S 1974 *Practical Quantum Mechanics* (Berlin: Springer) 0387070508
[3] Ikhdair S M and Sever R 2007 *J. Math. Chem.* **41** 343
[4] Bahar M K and Soylu A 2018 *Phys. Plasmas* **25** 022106
[5] Bahar M K and Soylu A 2018 *Phys. Plasmas* **25** 062113
[6] Munjal D and Prasad V 2017 *Contrib. Plasma Phys.* **57** 76
[7] Varshni Y P 1990 *Phys. Rev.* A **41** 4682
[8] Arda A, Aydoğdu O and Sever R 2011 *Phys. Scr.* **84** 025004
[9] Bahlouli H, Abdelmonem M S and Al-Marzoug S M 2012 *Chem. Phys.* **393** 153
[10] Bahar M K, Soylu A and Poszwa A *IEEE Trans. Plasma Sci.* **44** 2297
[11] Bahar M K and Soylu A 2018 *J. Phys. B: At. Mol. Opt. Phys.* **51** 105701
[12] Ikhdair S M and Sever R 2007 *J. Math. Chem.* **42** 461
[13] Aktaş M and Sever R 2004 *J. Mol. Struct. (Theochem)* **710** 223
[14] Gu X-Y, Zhang M and Sun J-Q 2010 *Chin. J. Phys.* **48** 222 (https://ps-taiwan.org/cjp/issues.php?vol=48&num=2)
[15] Setare M R and Karimi E 2007 *Int. J. Theor. Phys.* **46** 1381
[16] Sever R, Tezcan C, Yeşiltaş Ö and Bucurgat M 2008 *Int. J. Theor. Phys.* **47** 2243
[17] Mercero J M, Fowler J E, Sarasola C and Ugalde J M 1998 *Phys. Rev.* A **57** 2550
[18] Bertini L, Mella M, Bressanini D and Morosi G 2004 *Phys. Rev.* A **69** 042504
[19] Núñez M A 1993 *Phys. Rev.* A **47** 3620
[20] Stubbins C 1993 *Phys. Rev.* A **48** 220
[21] Ugalde J M, Sarasola C and Lopez X 1997 *Phys. Rev.* A **56** 1642
[22] Dong S-H, Sun G-H and L-Cassou M 2004 *Phys. Lett.* A **328** 299
[23] Dong S-H, Chen C-Y and L-Cassou M 2005 *Int. J. Quant. Chem.* **105** 453
[24] Ikhdair S M 2008 *Int. J. Mod. Phys.* C **19** 1425
[25] Ikhdair S M and Sever R 2008 *Cent. Eur. J. Phys.* **6** 685
[26] Ikhdair S M 2008 *Int. J. Mod. Phys.* C **19** 221
[27] Rajabi A A and Hamzavi M 2013 *J. Theor. Appl. Phys.* **7** 17
[28] Zhang M-C, Sun G-H and Dong S-H 2010 *Phys. Lett.* A **374** 704
[29] Sadeghi J, Rostami M and Hojabri A R 2009 *Int. J. Theor. Phys.* **48** 2961
[30] Zhang M-C 2009 *Int. J. Theor. Phys.* **48** 2625
[31] Chen C-Y and Dong S-H 2005 *Phys. Lett.* A **335** 374
[32] Antia A D, Umo E E A and Umoren C C 2015 *J. Theor. Phys. Cryptogr.* **10** 1 (http://ijtpc.ir/volume10/JTPC2114.pdf)
[33] Aktaş M and Sever R 2005 *J. Math. Chem.* **37** 139

[34] Berkdemir C and Cheng Y-F 2009 *Phys. Scr.* **79** 035003
[35] Berkdemir C 2009 *J. Math. Chem.* **46** 139
[36] Parmar R H 2019 *Eur. Phys. J. Plus* **134** 86
[37] Mbadjoun B T, Ema'a J M E, Yomi J, Abiama P E, B-Bolie G H and Ateba P O 2019 *Mod. Phys. Lett.* A **34** 1950072
[38] Cheng Y F and Dai T Q 2007 *Phys. Scr.* **75** 274
[39] Agboola D 2011 *Commun. Theor. Phys.* **55** 972
[40] Ikot A N, Olgar E and Hassanabadi H 2016 *Gazi Univ. J. Sci.* **29** 937 (http://ijtpc.ir/volume10/JTPC2114.pdf)
[41] Amirfakhrian M and Hamzavi M 2012 *Mol. Phys.* **110** 2173
[42] Chen C-Y, Lu F-L, Sun D-S, You Y and Dong S-H 2016 *Ann. Phys.* **371** 183
[43] Liu G and Guo K 2012 *Superlattices Microstruct.* **52** 997
[44] Chen C-Y, You Y, Wang X-H and Dong S-H 2013 *Phys. Lett.* A **377** 1521
[45] Khordad R 2017 *Opt. Commun.* **391** 121
[46] Wang Z, Long Z-W, Long C-Y and Teng J 2015 *Phys. Scr.* **90** 055201
[47] Hassanabadi H, Ikot A N and Zarrinkamar S 2014 *Acta Phys. Pol.* A **126** 647
[48] Liu G, Guo K, Hassanabadi H, Lu L and Yazarloo B H 2013 *Physica* B **415** 92
[49] Khordad R 2017 *Superlattices Microstruct.* **110** 146
[50] Nautiyal V V and Silotia P 2018 *Phys. Lett.* A **382** 2061
[51] Chabab M, Lahbas A and Oulne M 2015 *Eur. Phys. J.* A **51** 131
[52] Chen C-Y, Sun D-S and Lu F-L 2006 *Phys. Lett.* A **348** 153
[53] Stevanović L 2010 *J. Phys. B: At. Mol. Opt. Phys.* **43** 165002
[54] Kumar A, Kumar M and Meath W J 2003 *Chem. Phys.* **286** 227
[55] Zhang Y-H, Tang L-Y, Zhang X-Z, Shi T-Y and Mitroy J 2012 *Chin. Phys. Lett.* **29** 063101
[56] Mitroy J, Safronova M S and Clark C W 2010 *J. Phys. B: At. Mol. Opt. Phys.* **43** 202001
[57] Lumb S, Lumb S and Prasad V 2015 *Eur. Phys. J. Plus* **130** 149
[58] Borschevsky A, Zelovich T, Eliav E and Kaldor U 2012 *Chem. Phys.* **395** 104
[59] Ganguly J and Ghosh M 2015 *Chem. Phys.* **447** 54
[60] Çakır B, Yakar Y and Özmen A 2013 *Opt. Commun.* **311** 222
[61] Kang S, He J, Xu N and Chen C-Y 2014 *Commun. Theor. Phys.* **62** 881
[62] Scott R A and Lukehart C M (ed) 2007 *Applications of Physical Methods to Inorganic and Bioinorganic Chemistry* (New York: Wiley) p 361 978-0-470-032176
[63] Flores C M and C-Trujillo R 2018 *J. Phys. B: At. Mol. Opt. Phys.* **51** 055203
[64] Lumb S, Lumb S and Prasad V 2015 *Eur. Phys. J.* D **69** 176
[65] Lumb S, Lumb S, Munjal D and Prasad V 2015 *Phys. Scr.* **90** 095603
[66] Lumb S, Lumb S and Prasad V 2015 *Phys. Lett.* A **379** 1263
[67] Lumb S, Lumb S and Prasad V 2014 *Phys. Rev.* A **90** 032505
[68] Lumb S, Lumb S and Prasad V 2015 *Indian J. Phys.* **89** 13
[69] Hall R L 1992 *J. Phys. A: Math. Gen.* **25** 4459